

Comparison of the Structures and Properties of $[\text{N}(\text{C}_2\text{H}_5)_4][\text{Pt}\{\text{S}_2\text{C}_2(\text{CN})_2\}_2]$ and $[\text{H}_3\text{O}]_x[\text{NH}_4]_{1-x}[\text{Pt}\{\text{S}_2\text{C}_2(\text{CN})_2\}_2] \cdot 2 - x\text{H}_2\text{O}^*$

Peter I. Clemenson and Allan E. Underhill

Department of Chemistry and Institute of Molecular and Biomolecular Electronics, University College of North Wales, Bangor, Gwynedd LL57 2UW

Michael B. Hursthouse and Richard L. Short

Department of Chemistry, Queen Mary College, Mile End Road, London E1 4NS

The crystal structures of $[\text{N}(\text{C}_2\text{H}_5)_4][\text{Pt}\{\text{S}_2\text{C}_2(\text{CN})_2\}_2]$ and $[\text{H}_3\text{O}]_x[\text{NH}_4]_{1-x}[\text{Pt}\{\text{S}_2\text{C}_2(\text{CN})_2\}_2] \cdot 2 - x\text{H}_2\text{O}$ are described. Both compounds contain anion dimers. In the former the dimer has a slipped configuration with Pt...S interactions whereas the latter contains the anions in an eclipsed configuration with a Pt over Pt arrangement. The difference in the structures is related to the size and nature of the cation. The electrical conduction and magnetic properties are related to the structures.

The chemistry of the complexes of the ligand 1,2-dicyanoethylene-1,2-dithiolate has excited great interest amongst chemists for the past twenty years.¹⁻³ It was realised soon after their discovery that these complexes possessed unusual redox properties arising from the fact that the highest energy electrons occupied a delocalised molecular orbital involving both metal and ligand orbitals. More recently interest in these compounds has taken fresh impetus with the discovery of a new type of one-dimensional metal based on the platinum complex $[\text{H}_3\text{O}]_{0.33}\text{Li}_{0.8}[\text{Pt}\{\text{S}_2\text{C}_2(\text{CN})_2\}_2] \cdot 1.67\text{H}_2\text{O}$.^{4,5} Hoffmann and co-workers³ in a recent review article have pointed out the paucity of structural data on complexes of this type. They discussed in detail the mode of dimerisation observed in $\text{S}_2\text{C}_2(\text{CN})_2^{2-}$ complexes and explained the relative arrangement of anions in the lattice in terms of the minimisation of steric repulsion from lone pairs of electrons on the sulphur atoms.

In this paper we describe the crystal structures of $[\text{N}(\text{C}_2\text{H}_5)_4][\text{Pt}\{\text{S}_2\text{C}_2(\text{CN})_2\}_2]$ and $[\text{H}_3\text{O}]_x[\text{NH}_4]_{1-x}[\text{Pt}\{\text{S}_2\text{C}_2(\text{CN})_2\}_2] \cdot 2 - x\text{H}_2\text{O}$ and relate them to those of other $[\text{Pt}\{\text{S}_2\text{C}_2(\text{CN})_2\}_2]^-$ salts.

Experimental

$[\text{N}(\text{C}_2\text{H}_5)_4][\text{Pt}\{\text{S}_2\text{C}_2(\text{CN})_2\}_2]$ was prepared according to the method of Davidson and Holm.⁶ Black needle-shaped crystals were obtained upon slow crystallization or evaporation of a solution of the salt in dichloromethane (Found: C, 31.85, 32.05; H, 3.35, 3.45; N, 11.9, 11.9. Calc. for $\text{C}_{16}\text{H}_{20}\text{N}_5\text{PtS}_4$: C, 31.70; H, 3.30; N, 11.55%), m.p. 288 °C (decomp.) [lit.⁶ m.p., 288 °C (decomp.)].

$[\text{H}_3\text{O}]_x[\text{NH}_4]_{1-x}[\text{Pt}\{\text{S}_2\text{C}_2(\text{CN})_2\}_2] \cdot 2 - x\text{H}_2\text{O}$ was prepared by passing a 0.6 mmol dm⁻³ solution of $[\text{N}(\text{C}_2\text{H}_5)_4]_2[\text{Pt}\{\text{S}_2\text{C}_2(\text{CN})_2\}_2]$ in acetone-water (70:30) through an ion-exchange column in the acid form and allowing the resulting solution to mix with a solution of NH_4Cl (four-fold excess) in water. Slow evaporation of the resulting solution yielded a mixture of needle-shaped crystals and a microcrystalline material [Found: C, 18.45; H, 1.3; N, 13.45. Calc. for

Table 1. Fractional atomic co-ordinates ($\times 10^4$) for $[\text{N}(\text{C}_2\text{H}_5)_4][\text{Pt}\{\text{S}_2\text{C}_2(\text{CN})_2\}_2]$

Atom	x	y	z
Pt(1)	422(0.5)	509(0.5)	2 855(1)
S(1)	1 458(1)	1 224(2)	3 865(4)
S(2)	-192(1)	1 710(2)	1 810(4)
S(3)	1 046(2)	-679(2)	3 951(5)
S(4)	-598(2)	-235(2)	1 868(4)
N(1)	2 146(6)	3 374(8)	3 991(21)
N(2)	107(6)	3 956(7)	1 419(19)
N(3)	787(7)	-2 930(7)	4 247(19)
N(4)	-1 256(6)	-2 384(7)	1 587(18)
C(1)	1 187(5)	2 227(7)	3 276(15)
C(2)	479(5)	2 437(7)	2 345(15)
C(3)	1 718(7)	2 865(8)	3 706(19)
C(4)	272(6)	3 286(8)	1 835(18)
C(5)	395(6)	-1 405(7)	3 397(15)
C(6)	-305(6)	-1 233(6)	2 443(13)
C(7)	610(7)	-2 240(8)	3 807(20)
C(8)	-845(7)	-1 874(7)	1 963(17)
N(5)	1 866(4)	5 121(5)	9 344(12)
C(9)	1 597(6)	5 954(7)	8 270(18)
C(10)	2 146(7)	6 651(8)	8 847(24)
C(11)	1 229(6)	4 528(7)	8 828(18)
C(12)	882(7)	4 345(8)	6 695(22)
C(13)	2 435(6)	4 760(8)	8 630(19)
C(14)	2 723(7)	3 922(8)	9 483(23)
C(15)	2 171(6)	5 219(9)	11 552(16)
C(16)	1 683(9)	5 627(10)	12 434(22)

$\text{C}_8\text{H}_8\text{N}_5\text{O}_2\text{PtS}_4$ ($x = 0$): C, 18.15; H, 1.50; N, 13.25%]. The analysis of this compound varied from preparation to preparation. The N content was found to be as low as 11.4% in some samples (calc. for $x = 1$: N, 10.9%).

X-Ray Structure Determinations.—Crystals of the two compounds were mounted on glass fibres. Following preliminary photography, unit-cell parameters in each case were obtained by least-squares refinement of the setting angles for 25 automatically centred reflections measured on a CAD4 diffractometer. Intensities were recorded on the $\omega/2\theta$ scan mode with graphite monochromated Mo- K_α radiation ($\lambda = 0.710 69 \text{ \AA}$) following standard procedures as previously described in detail.⁷ Semi-empirical absorption corrections were applied in each case.⁸ The structures were solved *via* routine heavy-atom procedures and refined *via* application of full-matrix least

* Tetraethylammonium bis(1,2-dicyanoethylene-1,2-dithiolato)platinate(1-) and oxonium bis(1,2-dicyanoethylene-1,2-dithiolato)platinate(1-) hydrate.

Supplementary data available: see Instructions for Authors, *J. Chem. Soc., Dalton Trans.*, 1989, Issue 1, pp. xvii-xx.

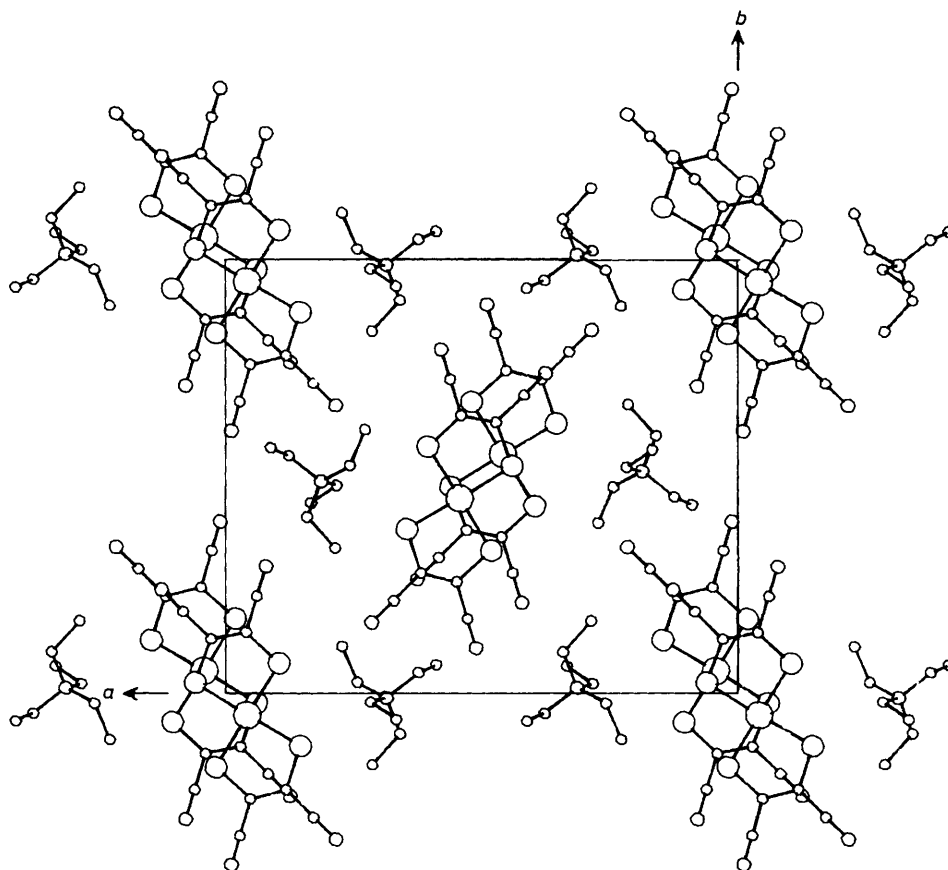


Figure 1. A projection of the structure of $[\text{N}(\text{C}_2\text{H}_5)_4][\text{Pt}\{\text{S}_2\text{C}_2(\text{CN})_2\}_2]$ as viewed along the c axis

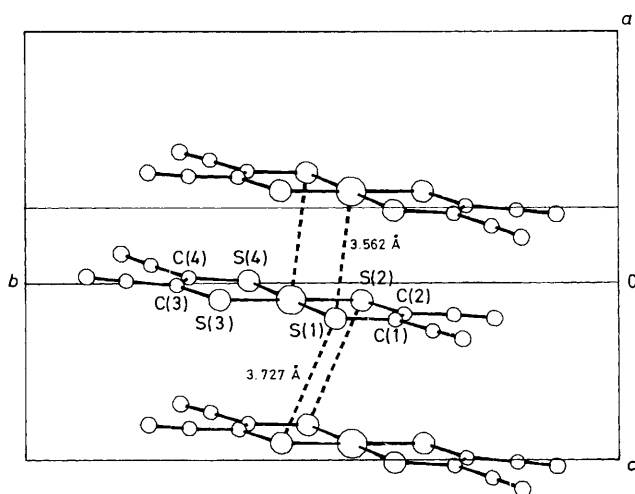


Figure 2. A projection of the structure of $[\text{N}(\text{C}_2\text{H}_5)_4][\text{Pt}\{\text{S}_2\text{C}_2(\text{CN})_2\}_2]$ showing the arrangement of anions in the dimer and the interdimer separation

squares. For the final refinements, a weighting scheme of the type $w = 1/[\sigma^2(F_o) + g(F_o)^2]$ was used. Atomic scattering factor data were taken from ref. 9 and all calculations were made using SHELX 76.¹⁰

Crystal data for $[\text{N}(\text{C}_2\text{H}_5)_4][\text{Pt}\{\text{S}_2\text{C}_2(\text{CN})_2\}_2]$. Black needles, $\text{C}_{16}\text{H}_{20}\text{N}_5\text{PtS}_4$, $M = 605.71$, monoclinic, space group

Table 2. Fractional atomic co-ordinates ($\times 10^4$) for $[\text{H}_3\text{O}][\text{Pt}\{\text{S}_2\text{C}_2(\text{CN})_2\}_2]\cdot\text{H}_2\text{O}$

Atom	x	y	z
Pt(1)	162(0.5)	2 736(1)	436(1)
S(1)	-1 203(2)	2 385(4)	1 643(4)
S(2)	-532(2)	1 699(4)	-2 785(4)
S(3)	1 524(2)	3 086(4)	-790(4)
S(4)	860(2)	3 748(4)	3 659(4)
C(1)	-1 932(7)	1 501(14)	-483(15)
C(2)	-1 645(7)	1 196(14)	-2 401(16)
C(10)	-2 869(7)	1 021(16)	-303(16)
N(1)	-3 622(7)	629(17)	-218(16)
C(20)	-2 291(8)	451(16)	-4 130(16)
N(2)	-2 837(7)	-158(17)	-5 454(16)
C(3)	2 261(7)	3 830(14)	1 370(16)
C(4)	1 981(7)	4 127(15)	3 303(16)
C(30)	3 205(7)	4 207(15)	1 186(16)
N(3)	3 974(7)	4 499(16)	1 104(16)
C(40)	2 648(8)	4 739(17)	5 011(16)
N(4)	3 221(7)	5 201(17)	6 326(16)
O(1)	-5 179(7)	-2 105(16)	-3 637(15)
O(2)	-4 624(7)	-1 987(15)	-7 512(16)

$P2_1/a$, $a = 20.052(3)$, $b = 16.099(3)$, $c = 7.188(3)$ Å, $\beta = 110.51(5)^\circ$, $U = 2 173.1$ Å³, $Z = 4$, $D_c = 1.852$ g cm⁻³, $\mu(\text{Mo-K}\alpha) = 65.7$ cm⁻¹, $F(000) = 1 172$. Total data recorded 4 312 ($1.5 \leq \theta \leq 25.0$), unique 3 835, observed $[I > 1.5\sigma(I)]$ 3 049. Number of parameters 237, g parameter 0.000 01, final $R = 0.0574$, $R' = 0.067$. Non-hydrogen atoms anisotropic, hydrogen atoms inserted in idealised positions with group

Table 3. Interatomic distances and interbond angles for $[\text{N}(\text{C}_2\text{H}_5)_4][\text{Pt}\{\text{S}_2\text{C}_2(\text{CN})_2\}_2]$

Bond lengths (Å)			
S(1)–Pt(1)	2.260(5)	S(2)–Pt(1)	2.274(5)
S(3)–Pt(1)	2.270(5)	S(4)–Pt(1)	2.260(5)
C(1)–S(1)	1.710(13)	C(2)–S(2)	1.722(12)
C(5)–S(3)	1.693(15)	C(6)–S(4)	1.712(12)
C(3)–N(1)	1.152(17)	C(4)–N(2)	1.137(16)
C(7)–N(3)	1.175(16)	C(8)–N(4)	1.126(16)
C(2)–C(1)	1.382(15)	C(3)–C(1)	1.433(16)
C(4)–C(2)	1.439(16)	C(6)–C(5)	1.356(15)
C(7)–C(5)	1.412(17)	C(8)–C(6)	1.449(17)
C(9)–N(5)	1.546(15)	C(11)–N(5)	1.534(15)
C(13)–N(5)	1.525(15)	C(15)–N(5)	1.496(14)
C(10)–C(9)	1.524(17)	C(12)–C(11)	1.475(18)
C(14)–C(13)	1.513(19)	C(16)–C(15)	1.492(19)

Bond angles (°)			
S(2)–Pt(1)–S(1)	90.2(2)	S(3)–Pt(1)–S(1)	89.1(2)
S(3)–Pt(1)–S(2)	179.0(1)	S(4)–Pt(1)–S(1)	178.6(1)
S(4)–Pt(1)–S(2)	91.2(2)	S(4)–Pt(1)–S(3)	89.5(2)
C(1)–S(1)–Pt(1)	103.0(4)	C(2)–S(2)–Pt(1)	102.3(5)
C(5)–S(3)–Pt(1)	102.4(5)	C(6)–S(4)–Pt(1)	103.0(5)
C(2)–C(1)–S(1)	122.3(9)	C(3)–C(1)–S(1)	118.4(9)
C(3)–C(1)–C(2)	119.3(11)	C(1)–C(2)–S(2)	122.1(9)
C(4)–C(2)–S(2)	117.1(9)	C(4)–C(2)–C(1)	120.8(11)
C(1)–C(3)–N(1)	177.7(15)	C(2)–C(4)–N(2)	179.5(12)
C(6)–C(5)–S(3)	123.7(10)	C(7)–C(5)–S(3)	117.1(10)
C(7)–C(5)–C(6)	119.0(12)	C(5)–C(6)–S(4)	121.4(9)
C(8)–C(6)–S(4)	116.5(9)	C(8)–C(6)–C(5)	122.1(11)
C(5)–C(7)–N(3)	176.5(15)	C(6)–C(8)–N(4)	178.7(13)
C(11)–N(5)–C(9)	107.7(9)	C(13)–N(5)–C(9)	109.4(9)
C(13)–N(5)–C(11)	109.8(9)	C(15)–N(5)–C(9)	112.3(10)
C(15)–N(5)–C(11)	108.6(9)	C(15)–N(5)–C(13)	109.0(9)
C(10)–C(9)–N(5)	114.2(10)	C(12)–C(11)–N(5)	115.2(11)
C(14)–C(13)–N(5)	115.1(11)	C(16)–C(15)–N(5)	114.3(11)

Selected intermolecular non-bonded distances (Å)			
Pt(1)–Pt(1a)	4.326	S(3)–Pt(1a)	4.330
S(4)–Pt(1b)	3.562	S(4)–S(3a)	3.727

Key to symmetry operations relating designated atoms to reference atoms at (x, y, z) : (a) $-x, -y, 1.0 - z$, (b) $-x, -y, -z$.

Table 4. Interatomic distances and interbond angles for $[\text{H}_3\text{O}][\text{Pt}\{\text{S}_2\text{C}_2(\text{CN})_2\}_2]\cdot\text{H}_2\text{O}$

Bond lengths (Å)			
S(1)–Pt(1)	2.266(4)	S(2)–Pt(1)	2.273(4)
S(3)–Pt(1)	2.269(4)	S(4)–Pt(1)	2.274(5)
Pt(1)–Pt(1a)	3.447(4)	C(1)–S(1)	1.696(12)
C(2)–S(2)	1.714(12)	C(3)–S(3)	1.698(13)
C(4)–S(4)	1.706(12)	C(2)–C(1)	1.392(15)
C(10)–C(1)	1.425(15)	C(20)–C(2)	1.425(15)
N(1)–C(10)	1.136(15)	N(2)–C(20)	1.140(15)
C(4)–C(3)	1.396(15)	C(30)–C(3)	1.423(15)
C(40)–C(4)	1.414(15)	N(3)–C(30)	1.147(15)
N(4)–C(40)	1.140(15)		

Bond angles (°)			
S(2)–Pt(1)–S(1)	90.3(2)	S(3)–Pt(1)–S(1)	179.7
S(3)–Pt(1)–S(2)	89.4(2)	S(4)–Pt(1)–S(1)	89.8(2)
S(4)–Pt(1)–S(2)	179.5(1)	S(4)–Pt(1)–S(3)	90.5(2)
C(1)–S(1)–Pt(1)	102.8(4)	C(2)–S(2)–Pt(1)	102.0(5)
C(3)–S(3)–Pt(1)	102.1(5)	C(4)–S(4)–Pt(1)	102.4(5)
C(2)–C(1)–S(1)	122.3(9)	C(10)–C(1)–S(1)	119.1(9)
C(10)–C(1)–C(2)	118.6(10)	C(1)–C(2)–S(2)	122.1(9)
C(20)–C(2)–S(2)	117.9(9)	C(20)–C(2)–C(1)	119.7(10)
N(1)–C(10)–C(1)	178.0(12)	N(2)–C(20)–C(2)	176.8(11)
C(4)–C(3)–S(3)	123.2(9)	C(30)–C(3)–S(3)	118.1(9)
C(30)–C(3)–C(4)	118.7(10)	C(3)–C(4)–S(4)	121.8(9)
C(40)–C(4)–S(4)	119.2(9)	C(40)–C(4)–C(3)	119.0(10)
N(3)–C(30)–C(3)	177.7(12)	N(4)–C(40)–C(4)	176.4(12)

Selected intermolecular non-bonded distances (Å)			
S(1)–Pt(1c)	4.235	S(2)–Pt(1d)	3.793
S(3)–Pt(1c)	4.011	S(4)–Pt(1c)	4.189
S(1)–S(1d)	5.512	S(2)–S(1d)	4.095
S(3)–S(1c)	3.444	S(4)–S(1f)	3.866
S(4)–S(2b)	3.722	S(1)–S(3d)	3.904
S(2)–S(2e)	4.099	S(3)–S(2d)	4.726
S(4)–S(2c)	3.467	S(2)–S(4d)	3.887
S(4)–S(4f)	3.690		

Key to symmetry operations relating designated atoms to reference atoms at (x, y, z) : (b) $x, y, 1.0 + z$, (c) $-x, 1.0 - y, -z$, (d) $-x, -y, -z$, (e) $-x, -y, -1.0 - z$, (f) $-x, 1.0 - y, 1.0 - z$.

isotropic U values. Final fractional atomic co-ordinates are given in Table 1.

Crystal data for $[\text{H}_3\text{O}]_x[\text{NH}_4]_{1-x}[\text{Pt}\{\text{S}_2\text{C}_2(\text{CN})_2\}_2]_2 \cdot 2 - x\text{H}_2\text{O}$. Black needles, $\text{C}_8\text{H}_5\text{N}_4\text{O}_2\text{PtS}_4$ (the X -ray structure is consistent with $x \approx 1$ for the crystal studied), $M = 511.5$, triclinic, space group $P\bar{1}$, $a = 14.699(5)$, $b = 7.128(3)$, $c = 6.688(3)$ Å, $\alpha = 97.95(3)$, $\beta = 97.04(3)$, $\gamma = 93.26(3)^\circ$, $U = 695.5$ Å³, $Z = 2$, $D_c = 2.442$ g cm⁻³, $D_m = 2.456$ g cm⁻³, $\mu = 102.55$ cm⁻¹, $F(000) = 478$. Total unique data measured 2 429 ($1.5 \leq \theta \leq 25.0^\circ$), observed $[I > 1.5\sigma(I)]$ 2 220. Number of parameters 185, g parameter 0.000 05, final $R = 0.041$, $R' = 0.051$. Non-hydrogen atoms anisotropic, possible hydrogens detected on $\Delta\rho$ maps (but only two on each oxygen) and included with free positional refinement but assigned group U_{iso} values. Final fractional atomic co-ordinates are given in Table 2.

Additional material available from the Cambridge Crystallographic Data Centre comprises H-atom co-ordinates and thermal parameters.

Conductivity.—Conductivity measurements were made by the four-probe d.c. technique using a computer-controlled apparatus. Colloidal graphite was used as the contact material between the gold wires and the crystal.

Results and Discussion

Structure of $[\text{N}(\text{C}_2\text{H}_5)_4][\text{Pt}\{\text{S}_2\text{C}_2(\text{CN})_2\}_2]$.—Figure 1 shows the c axis projection of the crystal structure. The $[\text{Pt}\{\text{S}_2\text{C}_2(\text{CN})_2\}_2]^-$ anion is almost planar with average bond lengths Pt–S 2.267 and S–C 1.708 Å (Table 3). The planar anions are arranged in columns parallel to the a axis of the unit cell. The columns are surrounded by the bulky cation and the closest intercolumnar contact is between the CN groups of adjacent anions in the b direction or between the CN group of one anion and the S of an adjacent anion. Figure 2 shows the anion columns to consist of dimers. Figures 1 and 2 show that within the dimer the anions are in a slipped configuration such that the metal atom at the centre of each molecule is positioned above the S atom of the other molecule. The closest intradimer contact within the dimer species is the Pt–S distance of 3.562 Å whilst the shortest interdimer contact in the a direction is between the S atoms (3.727 Å).

The crystal structure is very similar to that found for $[\text{N}(\text{C}_2\text{H}_5)_4][\text{Ni}\{\text{S}_2\text{C}_2(\text{CN})_2\}_2]$.¹¹ In particular the intradimer contact of 3.562 Å for the Pt complex is similar to the average intraplanar spacing reported for the Ni complex (3.5 Å).¹¹

Structure of $[\text{H}_3\text{O}]_x[\text{NH}_4]_{1-x}[\text{Pt}\{\text{S}_2\text{C}_2(\text{CN})_2\}_2]_2 \cdot 2 - x\text{H}_2\text{O}$.—As discussed in the Experimental section the analysis of this product varied from preparation to preparation

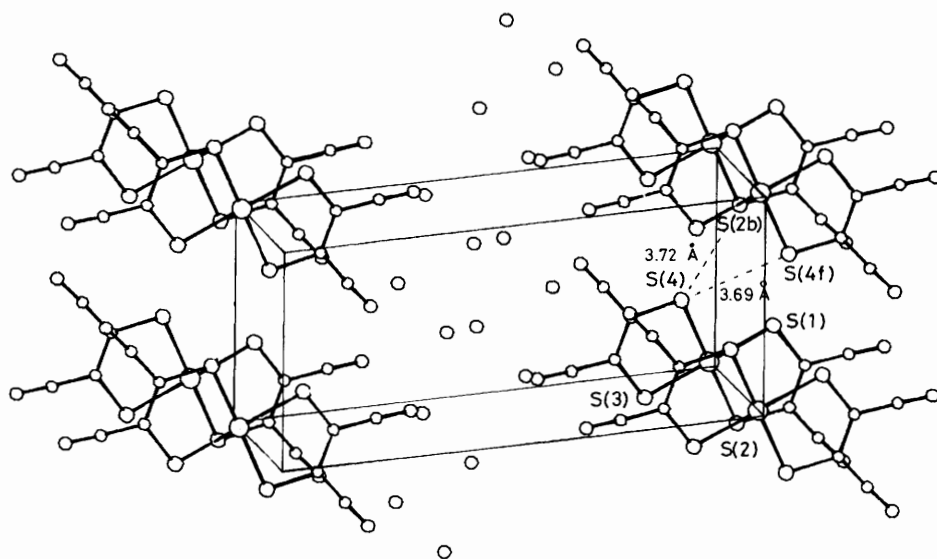


Figure 3. A projection of the structure of $[\text{H}_3\text{O}][\text{Pt}\{\text{S}_2\text{C}_2(\text{CN})_2\}_2]\cdot\text{H}_2\text{O}$ along the b^* axis

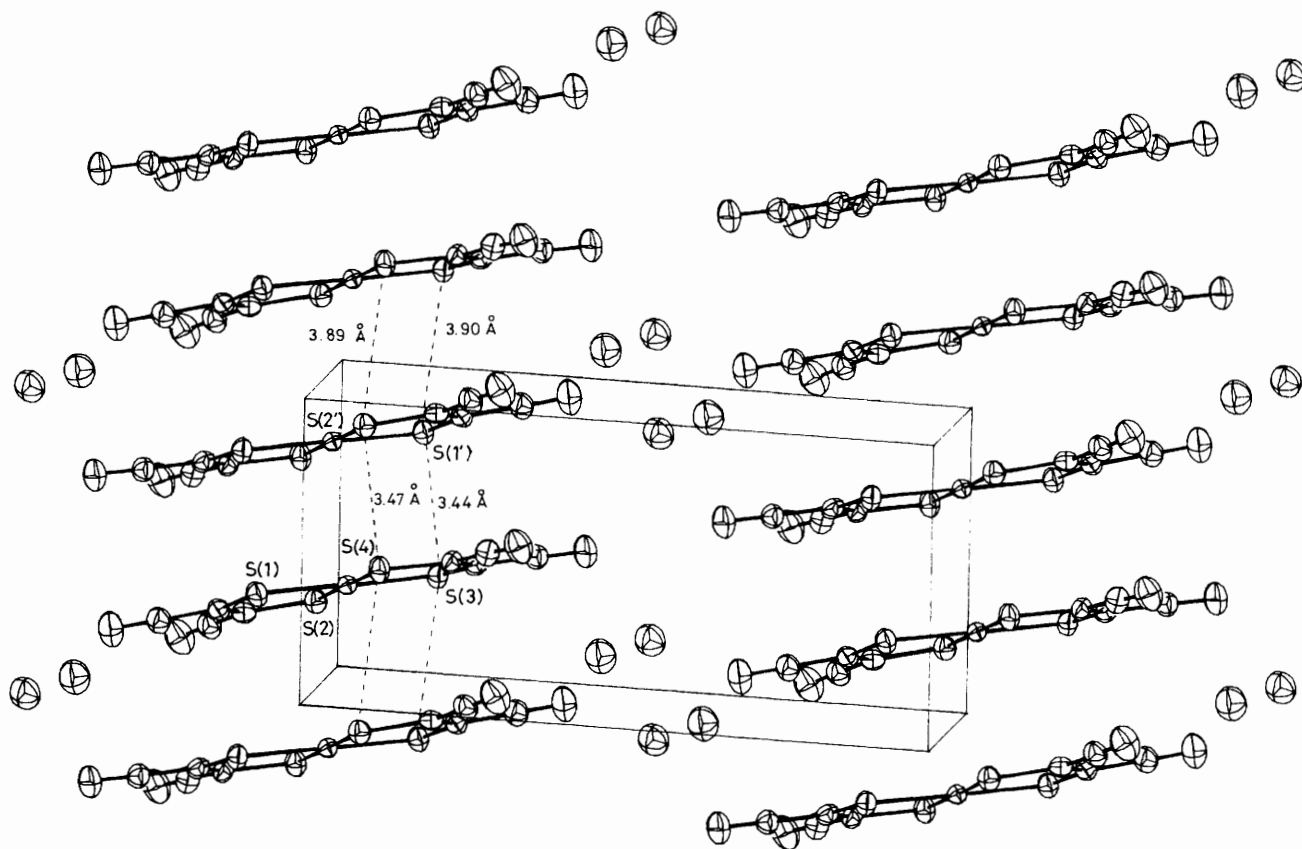


Figure 4. Crystal structure of $[\text{H}_3\text{O}][\text{Pt}\{\text{S}_2\text{C}_2(\text{CN})_2\}_2]\cdot\text{H}_2\text{O}$ showing the dimer unit

indicating that replacement of $[\text{NH}_4]^+$ by $[\text{H}_3\text{O}]^+$ could occur during preparation. The structure of the crystal used in the X-ray study could only be satisfactorily refined assuming the stoichiometry $[\text{H}_3\text{O}][\text{Pt}\{\text{S}_2\text{C}_2(\text{CN})_2\}_2]\cdot\text{H}_2\text{O}$. The $[\text{H}_3\text{O}]^+$ unit is believed to occupy the same position as the Rb^+ ion in $\text{Rb}[\text{Pt}\{\text{S}_2\text{C}_2(\text{CN})_2\}_2]\cdot\text{H}_2\text{O}$.¹²

Figure 3 shows the b^* projection of the crystal structure of $[\text{H}_3\text{O}][\text{Pt}\{\text{S}_2\text{C}_2(\text{CN})_2\}_2]\cdot\text{H}_2\text{O}$. The anions are arranged face

to face in an eclipsed configuration to form a columnar stacked structure. Figure 4 shows the c^* projection and reveals that within the stack the anions associate to give dimers, the $\text{S}\cdots\text{S}$ contacts within the dimer being 3.45, 3.46 Å, and between dimers 3.89 and 3.90 Å. The corresponding distances in the analogous $\text{Rb}[\text{Pt}\{\text{S}_2\text{C}_2(\text{CN})_2\}_2]\cdot\text{H}_2\text{O}$ are 3.43, 3.46 and 3.88, 3.91 Å.¹²

Between the columnar stacks of anions in the c direction there

are a number of short S-S contacts (Table 4). The arrangement of the stacks in the *c* direction and the intrastack distances are comparable to those found in $\text{Rb}[\text{Pt}\{\text{S}_2\text{C}_2(\text{CN})_2\}_2]\cdot\text{H}_2\text{O}$ ¹² and $[\text{H}_3\text{O}]_{0.33}\text{Li}_{0.8}[\text{Pt}\{\text{S}_2\text{C}_2(\text{CN})_2\}_2]\cdot 1.67\text{H}_2\text{O}$.⁵ This arrangement gives rise to a sheet like structure parallel to the *bc* plane. These sheets of anions are separated by the cations and water molecules (see Figure 3) which form a hydrogen-bonded network to the nitrogen atom of the cyano group on the ligands. The arrangement of the sheets in $[\text{H}_3\text{O}]_x[\text{NH}_4]_{1-x}[\text{Pt}\{\text{S}_2\text{C}_2(\text{CN})_2\}_2]\cdot 2-x\text{H}_2\text{O}$ is thus similar to that found in both $\text{Rb}[\text{Pt}\{\text{S}_2\text{C}_2(\text{CN})_2\}_2]\cdot\text{H}_2\text{O}$ ¹² and $[\text{H}_3\text{O}]_{0.33}\text{Li}_{0.8}[\text{Pt}\{\text{S}_2\text{C}_2(\text{CN})_2\}_2]\cdot 1.67\text{H}_2\text{O}$.⁵

Electrical Conductivity Studies.—The electrical conductivities have been determined down the needle axes of crystals of both compounds. In both cases this corresponds to the stacking direction of the columns of anions. The room temperature conductivity of $[\text{H}_3\text{O}]_x[\text{NH}_4]_{1-x}[\text{Pt}\{\text{S}_2\text{C}_2(\text{CN})_2\}_2]\cdot 2-x\text{H}_2\text{O}$ was $\approx 10^{-5} \Omega^{-1} \text{cm}^{-1}$. Over the temperature range 310–240 K it was found to behave as a semiconductor with an activation energy of 405 meV. The room temperature conductivity is similar to that reported for $\text{Rb}[\text{Pt}\{\text{S}_2\text{C}_2(\text{CN})_2\}_2]\cdot\text{H}_2\text{O}$ ($2.5 \times 10^{-5} \Omega^{-1} \text{cm}^{-1}$) whilst the activation energy is somewhat larger (300 ± 5 meV above 250 K and 240 ± 5 meV below 240 K).¹²

The value for the room temperature conductivity ($10^{-8} \Omega^{-1} \text{cm}^{-1}$) found for $[\text{N}(\text{C}_2\text{H}_5)_4][\text{Pt}\{\text{S}_2\text{C}_2(\text{CN})_2\}_2]$ is in good agreement with that reported previously.¹³ The similarity in the electrical conduction behaviour of these compounds in spite of the differences in the overlap within the dimer is probably due to the conductivity being limited by the interdimer hopping process rather than intradimer transfer.

Magnetic Properties.—The magnetic properties of $[\text{N}(\text{C}_2\text{H}_5)_4][\text{Pt}\{\text{S}_2\text{C}_2(\text{CN})_2\}_2]$ and $[\text{H}_3\text{O}]_x[\text{NH}_4]_{1-x}[\text{Pt}\{\text{S}_2\text{C}_2(\text{CN})_2\}_2]\cdot 2-x\text{H}_2\text{O}$ are quite different. Weiber *et al.*¹⁴ have shown that the $[\text{N}(\text{C}_2\text{H}_5)_4]^+$ salt is paramagnetic at room temperature (μ_{eff} 1.15) and becomes diamagnetic at low temperature. The temperature dependence of the susceptibility was shown to be consistent with a triplet-singlet equilibrium with a *J* value of 350cm^{-1} . On the other hand the $[\text{H}_3\text{O}]^+ / [\text{NH}_4]^+$ salt is diamagnetic at room temperature. When heated above room temperature the compound becomes slowly paramagnetic. The origin of this phenomenon is not understood at present and is being investigated further.¹⁵

General Discussion.—There has recently been a discussion of the reasons for the observation that, until the present study, only M-S dimers had been observed for nickel dithiolene complexes and M-M dimers for platinum dithiolene complexes. It was proposed that the choice between the two alternative dimeric structures relied on a delicate balance between M-S or M-M bonding and interring repulsions.³ The structures reported here add significant new results to this discussion. The results outlined here show that the differences observed in the two compounds described above are due to the influence of the cation on the crystal structure and not due to orbital overlap considerations. The $[\text{N}(\text{C}_2\text{H}_5)_4]^+$ cation differs from Rb^+ or $[\text{H}_3\text{O}]^+ / [\text{NH}_4]^+$ cations in two important ways. First, the

cation size is much larger and the slipped dimer arrangement found for this salt produces cavities in the lattice in which the cation can be accommodated. The $[\text{N}(\text{C}_2\text{H}_5)_4]^+$ salt is also anhydrous in contrast to the salts of small cations which are hydrated. In the latter structures and in that found for $[\text{H}_3\text{O}]_{0.33}\text{Li}_{0.8}[\text{Pt}\{\text{S}_2\text{C}_2(\text{CN})_2\}_2]\cdot 1.67\text{H}_2\text{O}$ the water molecules appear to play a role in bonding together the two-dimensional sheets of sulphur-sulphur anions described earlier. Thus the difference in the two types of structure appears to be dominated by interdimer rather than intradimer interactions.

The magnetic results clearly show that the Pt over Pt arrangement within the dimer leads to much stronger intermolecular overlap than the metal over sulphur arrangement. In the isolated monoanion the unpaired electron is located in a delocalised molecular orbital formed by the overlap of the Pt d_{xz} orbital with the ligand π orbital. The negative charge is distributed between the metal and the ligand with a significant amount on the sulphur atom. The short S-S and Pt-Pt distances are significantly shorter than the Pt-S separation in the $[\text{NH}_4]^+$ salt and provide an efficient exchange mechanism to produce the singlet ground state.

Acknowledgements

We would like to thank the S.E.R.C. for support and Johnson Matthey plc for the loan of platinum salts.

References

- 1 J. S. Miller and A. J. Epstein, *Prog. Inorg. Chem.*, 1976, **20**, 1.
- 2 J. A. McCleverty, *Prog. Inorg. Chem.*, 1968, **10**, 49.
- 3 S. Alvarez, R. Vicente, and R. Hoffmann, *J. Am. Chem. Soc.*, 1985, **107**, 6253.
- 4 A. E. Underhill and M. M. Ahmad, *J. Chem. Soc., Chem. Commun.*, 1981, 67; M. M. Ahmad, O. J. Turner, A. E. Underhill, C. S. Jacobson, K. Mortensen, and K. Carneiro, *Phys. Rev. B*, 1984, **29**, 4796.
- 5 A. Kobayashi, Y. Kobayashi, H. Kobayashi, A. E. Underhill, and M. M. Ahmad, *J. Chem. Soc., Chem. Commun.*, 1982, 390; A. Kobayashi, T. Mori, Y. Sasaki, H. Kobayashi, M. M. Ahmad, and A. E. Underhill, *Bull. Chem. Soc. Jpn.*, 1984, **57**, 3262.
- 6 A. Davidson and R. H. Holm, *Inorg. Synth.*, 1967, **10**, 8.
- 7 M. B. Hursthouse, R. A. Jones, K. M. A. Malik, and G. Wilkinson, *J. Am. Chem. Soc.*, 1979, **101**, 4128.
- 8 A. C. T. North, D. C. Phillips, and F. S. Matthews, *Acta Crystallogr., Sect. A*, 1968, **24**, 351.
- 9 'International Tables for X-Ray Crystallography,' Kynoch Press, Birmingham, 1974, vol. 4.
- 10 G. M. Sheldrick, SHELX 76, University of Cambridge, 1976.
- 11 A. Kobayashi and Y. Sasaki, *Bull. Chem. Soc. Jpn.*, 1977, **50**, 2650.
- 12 M. M. Ahmad, D. J. Turner, A. E. Underhill, A. Kobayashi, Y. Sasaki, and H. Kobayashi, *J. Chem. Soc., Dalton Trans.*, 1984, 1759.
- 13 M. M. Ahmad and A. E. Underhill, *J. Chem. Soc., Dalton Trans.*, 1983, 165.
- 14 J. F. Weiber, L. R. Melby, and R. E. Benson, *J. Am. Chem. Soc.*, 1964, **86**, 4329.
- 15 G. J. Ashwell, I. M. Sandy, P. I. Clemenson, and A. E. Underhill, unpublished work.

Received 16th March 1988; Paper 8/01101J